

See discussions, stats, and author profiles for this publication at: <https://www.researchgate.net/publication/259699192>

Above-room-temperature ferroelastic phase transition in a perovskite-like compound $[N(CH_3)_4][Cd(N_3)_3]$

ARTICLE *in* CHEMICAL COMMUNICATIONS · JANUARY 2014

Impact Factor: 6.83 · DOI: 10.1039/c3cc48581a · Source: PubMed

CITATIONS

14

READS

53

8 AUTHORS, INCLUDING:



Zi-Yi Du

Gannan Normal University

55 PUBLICATIONS 655 CITATIONS

SEE PROFILE



Wei-Xiong Zhang

Sun Yat-Sen University

84 PUBLICATIONS 3,850 CITATIONS

SEE PROFILE



Hao-Long Zhou

Sun Yat-Sen University

18 PUBLICATIONS 234 CITATIONS

SEE PROFILE



Xiao-Ming Chen

Sun Yat-Sen University

419 PUBLICATIONS 22,199 CITATIONS

SEE PROFILE

Above-room-temperature ferroelastic phase transition in a perovskite-like compound $[\text{N}(\text{CH}_3)_4][\text{Cd}(\text{N}_3)_3]^{\dagger}$

Cite this: *Chem. Commun.*, 2014, 50, 1989

Received 10th November 2013,
Accepted 16th December 2013

DOI: 10.1039/c3cc48581a

www.rsc.org/chemcomm

Zi-Yi Du,^{a,b} Ying-Ping Zhao,^b Wei-Xiong Zhang,^{*a} Hao-Long Zhou,^a Chun-Ting He,^a Wei Xue,^a Bao-Ying Wang^a and Xiao-Ming Chen^a

A new perovskite-like compound $[\text{N}(\text{CH}_3)_4][\text{Cd}(\text{N}_3)_3]$ is reported here, which undergoes a series of reversible phase transitions including an above-room-temperature ferroelastic phase transition. An order–disorder mechanism is found in these structural transitions owing to the sway of the rod-like N_3^- bridges as well as the rotation of the tetrahedron-like $[\text{N}(\text{CH}_3)_4]^+$ guests.

During the past decade, ferroelastic materials have attracted special attention, owing to their significant role in the design and exploitation of multiferroic materials and their promising potential applications such as piezoelectric sensors and mechanical switches.^{1–6} As the mechanical equivalent of ferromagnetism and ferroelectricity in ferroic materials, ferroelasticity is a phenomenon in which a material could exhibit spontaneous strain.⁴ When stress is applied to a ferroelastic material, a phase transition will occur in the material from one phase to an equally stable phase, either of a different crystal structure or of a different orientation (a “twin” phase), and the strain–stress relationship shows a hysteresis behaviour. Most ferroelastic materials show phase transition from a paraelastic phase to a ferroelastic phase with decreasing temperature. As it is rather a difficult experimental task to measure ferroelastic hysteresis with any acceptable degree of accuracy, it has become customary to call a material “ferroelastic” if a phase transition occurs (or may be thought to occur) which may conceivably generate ferroelasticity.⁷ Theoretically, such phase transitions should belong to the 94 species ferroelastic phase transitions which are deduced by Aizu.⁸

Ferroelastic materials have been initially found in some inorganic oxides such as $\text{Gd}_2(\text{MoO}_4)_3$ and BaTiO_3 ,^{9,10} and recently a few organic co-crystals with ferroelastic phase transitions have also been reported.^{6,11,12} Compared with conventional inorganic

ferroelastics, hybrid coordination polymers (CPs) take advantage of the structural tunability to develop new types of ferroelastics with multi-functional properties. Among many types of the various CPs, the quite unique perovskite-like CPs, which are assembled by the inclusion of guest species into the well-matched host cages, may be very promising candidates for the construction of ferroelastic materials. Upon application of an external stimulus such as temperature or pressure, the induced order–disorder change of the guest cation in the well-designed cage-like frameworks can often be the dominant driving force for structural phase transitions. However, up to now, reports on such CPs have been very scarce.^{13–21} The ligands employed mainly contained the monoatomic I^- , diatomic CN^- , and multi-atomic HCOO^- and N_3^- anions, all of which acted as monovalent end-to-end bridging ligands.

In our current studies, we are interested in searching new types of ferroelastics in the perovskite-like CPs, and our efforts yielded such a compound $[\text{N}(\text{CH}_3)_4][\text{Cd}(\text{N}_3)_3]$ (**1**), which, to the best of our knowledge, is a new example of compounds exhibiting a unique ferroelastic phase transition, induced by the sway or rotation of the N_3^- bridges and the $[\text{N}(\text{CH}_3)_4]^+$ guests.

Compound **1** was synthesized as block-shaped single crystals from slow evaporation of the filtrate of a mixture of $\text{Cd}(\text{NO}_3)_2 \cdot 4\text{H}_2\text{O}$, NaN_3 and $(\text{CH}_3)_4\text{NBr}$ in the ratio of 1 : 12 : 6 (for experimental details and **Caution** statement see the ESI†). Compared with the somewhat unstable $\text{Mn}(\text{II})$ analogue,²¹ **1** is more stable when exposed to air, and the TGA curve shows that **1** can be stable up to 300 °C, whereupon a rapid decomposition occurs (Fig. S1, ESI†).

Differential scanning calorimetry (DSC) was used to detect the possible phase transitions and to confirm the existence of heat anomalies. As can be seen in Fig. 1, the DSC curves of **1** show two slightly overlapped peaks and one discrete endothermic peak at the heating run, as well as one single and two overlapped exothermic peaks at the cooling run, revealing that **1** undergoes three reversible phase transitions at $T_{\text{heating}}/T_{\text{cooling}}$ of 270/263, 277/270 and 322/318 K, respectively. For convenience, we labeled the phase below 270/263 K as the α phase, between 270/263 and 277/270 K as the β phase, between 277/270 and 322/318 K as the γ phase, and above 322/318 K as the δ phase. For the $\alpha \leftrightarrow \beta$ transition, the sharp peak and a

^a MOE Key Laboratory of Bioinorganic and Synthetic Chemistry, School of Chemistry & Chemical Engineering, Sun Yat-Sen University, Guangzhou, 510275, P. R. China. E-mail: zhangwx6@mail.sysu.edu.cn

^b College of Chemistry & Chemical Engineering, Gannan Normal University, Ganzhou 341000, P. R. China

† Electronic supplementary information (ESI) available: Experimental details and characterizations. CCDC 970021–970023. For ESI and crystallographic data in CIF or other electronic format see DOI: 10.1039/c3cc48581a

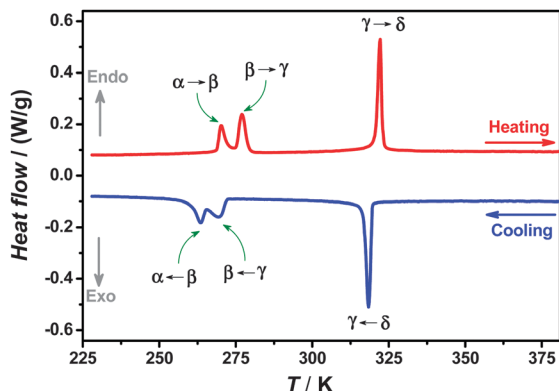


Fig. 1 DSC curves of **1** obtained on a heating–cooling cycle.

somewhat large thermal hysteresis of *ca.* 7 K between the heating and cooling runs reveal the discontinuous character of the transition, indicative of being a first-order phase transition. The similar first-order characteristics can also be observed for the $\beta \leftrightarrow \gamma$ and $\gamma \leftrightarrow \delta$ transitions.

In order to understand the phase transitions, the crystal structures of **1** were determined at different temperatures. The *in situ* variable-temperature X-ray diffraction analysis revealed that **1** crystallizes in the centrosymmetric space groups $C2/c$ at 220 K (α phase), $P2_1/m$ at 300 K (γ phase), and $Pm\bar{3}m$ at 350 K (δ phase), respectively (Table S1, ESI†). Because the β phase is located just between two very close phase transitions, its crystal structure is hard to be determined. These phase transitions are also clearly confirmed by the variable-temperature powder X-ray diffraction analysis (Fig. 2).

The crystal structure in all of these phases can be roughly described as a distorted perovskite-like structure, in accordance with a general formula of ABY_3 (the valence ratio of the cationic A, B and anionic Y components is 1:2:1). The Cd(II) ion is octahedrally coordinated to six nitrogen atoms through six azido ions, all of which act as end-to-end bridging ligands between two Cd(II) ions, thus leading to a three-dimensional cage-like framework. The common structural feature of **1** is the anionic $[\text{Cd}(\text{N}_3)_3]^-$ cage enclosed by twelve Cd–N–N–N–Cd fragments, within which the guest $[\text{N}(\text{CH}_3)_4]^+$ cation resides (Fig. 3).

The structural differences among α , γ and δ phases can mainly be attributed to the sway or rotation of the rod-like N_3^-

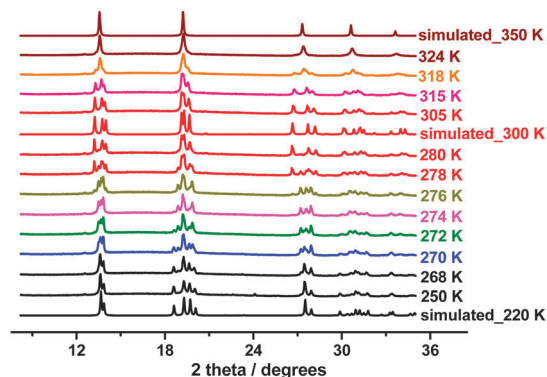


Fig. 2 Variable-temperature powder XRD patterns of **1**.

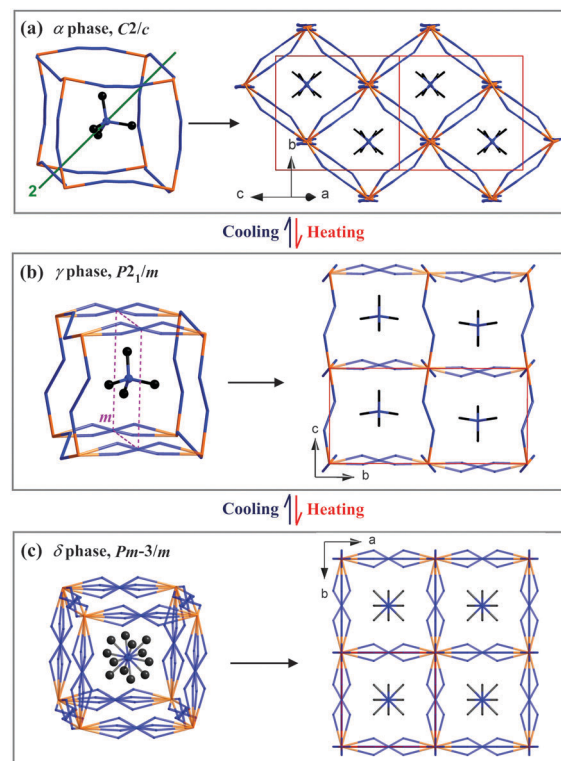


Fig. 3 Crystal structures of **1** at 220 K (a), 300 K (b), and 350 K (c). Cd, N and C atoms are shaded in orange, blue and black, respectively. Some of the N_3^- anions show disorder at 300 K, and all the N_3^- anions as well as the $[\text{N}(\text{CH}_3)_4]^+$ guests are disordered at 350 K.

bridges and the tetrahedron-like $[\text{N}(\text{CH}_3)_4]^+$ guest. As shown in Fig. 3, one and a half crystallographically independent N_3^- bridges in the α phase are ordered, whereas one of the three halves of crystallographically independent N_3^- in the γ phase sways slightly over two sites. In the δ phase, there exists only one independent N_3^- bridge and it blurs over four positions, as required by the pseudo-cubic imposed symmetry. By and large, the $[\text{Cd}(\text{N}_3)_3]^-$ cage exhibits high flexibility in a variety of symmetry elements, and its volume expands slightly from the α to γ phase, and further to the δ phase. As the temperature rises from 220 K to 350 K, the overall expansion of the volume is estimated to be 3.3%. On the other hand, both of the half crystallographically independent $[\text{N}(\text{CH}_3)_4]^+$ guests in α and γ phases are ordered and related by 2-fold axis and m mirror symmetries, respectively, whereas $[\text{N}(\text{CH}_3)_4]^+$ guests in the δ phase are located at the cage center, and become highly dynamically disordered, nearly over arbitrary orientation. Overall, the host–guest interaction accompanied with the synergic order–disorder transitions of the $[\text{Cd}(\text{N}_3)_3]^-$ cage and the $[\text{N}(\text{CH}_3)_4]^+$ guest during the heating/cooling process results in these structural phase transitions, and with the heating process, the cage units per cell decrease from four (in α phase) to two (in γ phase), and further to one (in δ phase).

It is noted that the unit cell parameters vary greatly from the α to γ phase [a , b , c (Å), β (°): 15.692(4), 8.8335(6), 9.529(6), 125.56(6) vs. 6.3264(3), 13.3644(6), 6.4349(3), 90.023(4)], and the monoclinic lattice type change from C to P during the heating process seems to be a relatively complicated transformation, and its mechanism is not clear enough for detailed discussion

yet, because the intermediate β phase is still unknown. Whereas for the transition from the δ to γ phase, it is clear that the total symmetric elements of the crystallographic point group decrease from 48 (E , $8C_3$, $3C_2$, $6C'_2$, $6C_4$, i , $8S_6$, $3\sigma_h$, $6\sigma_d$, and $6S_4$) to 4 (E , C_2 , i , and σ_h). Thus, this phase transition should be ferroelastic with an *Aizu* notation of $m3mF2/m(p)$,⁸ and the number of equivalent unique ferroelastic directions is up to 12. “ p ” in the parentheses means that the dyad axis of the ferroelastic crystal is along one of the tetrad axes of the prototype. The Curie symmetry principle tells us that the space group at the ferroelastic phase should be the sub-space group at the paraelastic phase, *i.e.* its maximal non-isomorphic sub-groups containing $\bar{1}$, $2/m$, mmm , $4/m$, $4/mmm$, $\bar{3}$, $\bar{3}m$, and $m3$, respectively. Furthermore, the number of spatial symmetry operations decrease from 48 to 4 during the symmetry breaking process (see Fig. S2, ESI†),²² in good agreement with macroscopic symmetry breaking.

The driving force for the $\alpha \rightarrow \gamma$ phase transition is mainly thought to be the cause of partial disorder of the N_3^- bridges, and the driving force for the $\gamma \rightarrow \delta$ transition can mainly be ascribed to the high disorder of the N_3^- bridges as well as the $[N(CH_3)_4]^+$ guests. The total entropy change (ΔS) in these phase transitions during the heating process can be estimated from the DSC measurements to be $20.11 \text{ J K}^{-1} \text{ mol}^{-1}$. From the Boltzmann equation, $\Delta S = R \ln N$, where N represents the ratio of possible configurations and R is the gas constant, it is found that $N \approx 11$. The large configuration value indicates an extremely high degree of disorder in the final δ phase, which originates from the dynamical rotation of the $[N(CH_3)_4]^+$ cation as well as the intense swing of the N_3^- anions. According to the theoretical calculations using *Materials Studio 5.0*,²³ the host-guest binding energy in **1** is a little higher than that in the Mn(II) analogue (-49.14 vs. $-34.13 \text{ kJ mol}^{-1}$), which is consistent with the fact that the ferroelastic phase transition temperature (T_c) in the former is obviously higher than that in the latter (322 vs. 303 K). It is also worthy of note that the Mn(II) analogue only undergoes one phase transition at above 173 K,^{13,21} whereas **1** can undergo three phase transitions at above 220 K. The nearest neighbouring Cd...Cd distances among the $[Cd(N_3)_3]^-$ cages vary slightly at different phases (Fig. S3, ESI†), and become equal in the cubic phase, being 6.523 Å at 350 K, which is longer than that of the Mn(II) analogue (6.451 Å at 333 K). We believe that the slightly larger metal ion radius of the Cd(II) ion in the present case leads to a greater freedom for structural transitions, reflecting that the subtle changes in the coordination parameters (*e.g.*, Mn–N 2.21 ~ 2.22 Å and Cd–N 2.32 ~ 2.35 Å) can modulate the flexibility of the perovskite-like azido-system, and tune its structural phase transitions.

The temperature dependence of the complex relative to dielectric permittivity was measured for **1** on a powder-pressed pellet at 100 kHz. Upon heating, both the real part (ϵ') and the imaginary part (ϵ'') of the dielectric permittivity show two obviously dielectric anomalies (Fig. S4, ESI†), which correspond to the phase transitions mentioned above. The dielectric permittivity varies significantly during the ferroelastic transition ($\gamma \leftrightarrow \delta$), compared with that during the transition between α and γ phases, implying that the former transition experiences larger changes in the dipole moments.

In conclusion, we have presented a new organic–inorganic hybrid compound with the perovskite-type architecture through

azido ligands and Cd(II) ions. It exhibits two very close transitions and one single reversible phase transition, with the latter being an above-room-temperature ferroelastic phase transition. An order-disorder mechanism is found in the structural transformations owing to the sway of the rod-like N_3^- bridges as well as the rotation of the tetrahedron-like $[N(CH_3)_4]^+$ guest at different temperatures. This compound represents a new class of ferroelastics as the perovskite-like CPs, shedding light on the understanding of the ferroic phase transitions for CPs and affording a useful strategy in the search for new ferroelastic materials. A detailed study is now underway.

This work was supported by the NSFC (21290173, 90922031, and 21121061), the 973 Project (2012CB821706), and the NSF of Guangdong (S2012030006240). W.-X. Z. is grateful to the SYSU for “100 Talents Program of SYSU” initial funding. Z.-Y. D. is thankful to the NSFC (21361002), and the China Postdoctoral Science Foundation funded project (2013M531888).

Notes and references

- 1 S. H. Baek, H. W. Jang, C. M. Folkman, Y. L. Li, B. Winchester, J. X. Zhang, Q. He, Y. H. Chu, C. T. Nelson, M. S. Rzechowski, X. Q. Pan, R. Ramesh, L. Q. Chen and C. B. Eom, *Nat. Mater.*, 2010, **9**, 309.
- 2 V. Nagarajan, A. Roytburd, A. Stanishevsky, S. Prasertchoung, T. Zhao, L. Chen, J. Melngailis, O. Auciello and R. Ramesh, *Nat. Mater.*, 2002, **2**, 43.
- 3 N. Balke, S. Choudhury, S. Jesse, M. Huijben, Y. H. Chu, A. P. Baddorf, L. Q. Chen, R. Ramesh and S. V. Kalinin, *Nat. Nanotechnol.*, 2009, **4**, 868.
- 4 E. K. H. Salje, *Annu. Rev. Mater. Res.*, 2012, **42**, 265.
- 5 M. C. Gallardo, J. Manchado, F. J. Romero, J. Cerro, E. K. H. Salje, A. Planes, E. Vives, R. Romero and M. Stipcich, *Phys. Rev. B*, 2010, **81**, 174102.
- 6 M. D. Hollingsworth, M. L. Peterson, J. R. Rush, M. E. Brown, M. J. Abel, A. A. Black, M. Dudley, B. Raghoebarachar, U. Werner-Zwanziger, E. J. Still and J. A. Vanecko, *Cryst. Growth Des.*, 2005, **5**, 2100.
- 7 E. K. H. Salje, *Contemp. Phys.*, 2000, **41**, 79.
- 8 K. Aizu, *J. Phys. Soc. Jpn.*, 1969, **27**, 387.
- 9 J. R. Barkley and W. Jeitschko, *J. Appl. Phys.*, 1973, **44**, 938.
- 10 T. Mitsui and J. Furuichi, *Phys. Rev.*, 1953, **90**, 193.
- 11 Y. Zhang, K. Awag, H. Yoshikawa and R.-G. Xiong, *J. Mater. Chem.*, 2012, **22**, 9841.
- 12 Z. Sun, X. Wang, J. Luo, S. Zhang, D. Yuan and M. Hong, *J. Mater. Chem. C*, 2013, **1**, 2561.
- 13 F. A. Mautner, R. Cortes, L. Lezama and T. Rojo, *Angew. Chem., Int. Ed.*, 1996, **35**, 78.
- 14 Z. Wang, B. Zhang, T. Otsuka, K. Inoue, H. Kobayashi and M. Kurmoo, *Dalton Trans.*, 2004, 2209.
- 15 P. Jain, N. S. Dalal, B. H. Toby, H. W. Kroto and A. K. Cheetham, *J. Am. Chem. Soc.*, 2008, **130**, 10450.
- 16 W. Zhang, Y. Cai, R.-G. Xiong, H. Yoshikawa and K. Awaga, *Angew. Chem., Int. Ed.*, 2010, **49**, 6608.
- 17 D.-W. Fu, W. Zhang, H.-L. Cai, Y. Zhang, R.-G. Xiong, S. D. Huang and T. Nakamura, *Angew. Chem., Int. Ed.*, 2011, **50**, 11947.
- 18 Y. Takahashi, R. Obara, Z.-Z. Lin, Y. Takahashi, T. Naito, T. Inabe, S. Ishibashi and K. Terakura, *Dalton Trans.*, 2011, **40**, 5563.
- 19 T. Asaji, Y. Ito, J. Seliger, V. Žagar, A. Gradišek and T. Apih, *J. Phys. Chem. A*, 2012, **116**, 12422.
- 20 W. Zhang, H.-Y. Ye, R. Graf, H. W. Spiess, Y.-F. Yao, R.-Q. Zhu and R.-G. Xiong, *J. Am. Chem. Soc.*, 2013, **135**, 5230.
- 21 X.-H. Zhao, X.-C. Huang, S.-L. Zhang, D. Shao, H.-Y. Wei and X.-Y. Wang, *J. Am. Chem. Soc.*, 2013, **135**, 16006.
- 22 *International tables for crystallography*, ed. T. Hahn, Springer, Dordrecht, Netherlands, 5th edn, 2002, vol. A.
- 23 *Accelrys, Materials Studio Getting Started, release 5.0*, Accelrys Software, Inc., San Diego, CA, 2009.